

Technetium-99m NGA Functional Hepatic Imaging: Preliminary Clinical Experience

Robert C. Stadalnik, David R. Vera, E. Steve Woodle, Walter L. Trudeau, Bruce A. Porter, Richard E. Ward, Kenneth A. Krohn,* and Lois F. O'Grady

Divisions of Nuclear Medicine, Gastroenterology, Diagnostic Radiology, Hematology-Oncology, Department of Surgery, University of California, Davis, Medical Center, Sacramento, California

Technetium-99m galactosyl-neoglycoalbumin ([Tc]NGA) is a radiolabeled ligand to hepatic binding protein, a receptor which resides at the plasma membrane of hepatocytes. This receptor-binding radiopharmaceutical and its kinetic model provide a noninvasive method for the assessment of liver function. Eighteen patients were studied: seven with hepatoma, eight with liver metastases, four with cirrhosis (two had concurrent hepatoma and one chronic active hepatitis), and one patient with acute fulminant non-A, non-B hepatitis. Technetium-99m NGA liver imaging provided anatomic information of diagnostic quality comparable to that obtained with other routine imaging modalities, including computed tomography, angiography, ultrasound, and [Tc]sulfur colloid scintigraphy. Kinetic modeling of dynamic [Tc]NGA data produced estimates of standardized hepatic blood flow, \bar{Q} (hepatic blood flow divided by total blood volume), and hepatic binding protein concentration, [HBP]. Clinical correlation was by classical Child-Turcotte criteria (CTC). Significant rank correlation was obtained between [HBP] estimates and CTC scores ($r_s = -0.72$, $p = 0.001$). This correlation supports the hypothesis that [HBP] is a measure of functional hepatocyte mass. The combination of decreased \bar{Q} and markedly reduced [HBP] may have prognostic significance; all three patients with this combination died of hepatic failure within 6 wk of imaging.

J Nucl Med 26:1233-1242, 1985

The development of a labeled hepatic binding protein [HBP] ligand, technetium-99m galactosyl-neoglycoalbumin ([Tc]NGA), and its kinetic model provide the basis for a unique functional imaging procedure for routine estimation of standardized hepatic blood flow \bar{Q} (hepatic blood flow divided by total blood volume) and hepatic binding protein concentration, [HBP].

Technetium-99m NGA is a member of a new class of tracers that, upon injection into the bloodstream, directs radioactivity to a selected tissue based upon chemical recognition and binding by a specific receptor molecule. Such radioligands can be used to probe the biochemistry of a receptor under various physiologic conditions (1).

Received Mar. 11, 1985; revision accepted June 14, 1985.

For reprints contact: Robert C. Stadalnik, MD, Div. of Nuclear Medicine, University of California, Davis, Med. Ctr., 2315 Stockton Blvd., CA 95817.

* Present address: Division of Nuclear Medicine, University of Washington Hospital, Seattle, WA.

Recent developments in cell biology have led to the discovery of receptor molecules which bind specific carbohydrate sequences of glycoproteins (2). The most extensively characterized of these receptors, HBP (3), resides at the cell surface of hepatocytes where it recognizes and binds galactose-terminated glycoproteins. After binding, the ligand-receptor complex is transported to hepatic lysosomes where the ligand is catabolized, and the receptor is subsequently recycled to the cell surface. Alteration of HBP binding has been demonstrated in specific physiologic and pathologic states (4-6). Based on the sensitivity of HBP biochemistry to hepatic function, we proposed this receptor as the target for a new receptor-binding radiopharmaceutical (7).

Preclinical studies in animals have confirmed the receptor-binding properties of [Tc]NGA (8). The agent is hepatocyte-specific, and its rate of accumulation depends upon the amount of ligand injected and its affinity for the receptor (8). Computer simulations of a

kinetic model for the hepatic uptake of the radiopharmaceutical indicate that a NGA of moderate affinity can be used to simultaneously estimate \bar{Q} and [HBP] from time-activity data (9).

The purpose of the present study was threefold: (a) to compare the diagnostic quality of [Tc]NGA liver images to those obtained by existing diagnostic imaging modalities; (b) to test the prognostic significance of the kinetic parameters, \bar{Q} and [HBP]; and (c) to test the hypothesis that [HBP] estimates by this technique are a measure of hepatocellular functional reserve.

MATERIALS AND METHODS

Radiopharmaceutical preparation

Preparation, labeling, and quality control of [Tc]NGA has been reported (7). The synthetic ligand was prepared by covalently coupling IME-thiogalactose to normal human serum albumin*. The molar ratio of these reagents controlled the number of galactose units per albumin molecule of the [Tc]NGA and thus provided a means for controlling the affinity of [Tc]NGA for HBP (9). Two carbohydrate densities were used in this study, 26 and 30 galactose units per albumin molecule, with HBP association constants of $5.5 \pm 1.5 \times 10^9 M^{-1}$ and $5.9 \pm 1.9 \times 10^9 M^{-1}$. The product was sterile (USP 71) and nonpyrogenic (USP 85, USP 151). The electrolytic method (10) was used to label NGA with technetium-99m (^{99m}Tc). High performance liquid chromatography (HPLC) (TSK-3000SW, 1.0 cc/min, 0.9% saline) was used to measure (NaI detector, 100–200 keV window; absorbance, 254 nm) labeling yield (the percent of protein-bound ^{99m}Tc) and the presence of polymeric [Tc]NGA. In all preparations, >98% of the radioactivity was protein bound; <2% was associated with polymeric NGA. Labeling and quality control could be accomplished in 1 hr.

Patient selection

The sole criterion for entrance into the study was that each patient have histologic evidence of liver disease. The protocol was approved by the University of California Davis Human Subjects Review Committee, and informed consent was obtained from each patient. Blood samples were obtained for CBC and blood chemistries within 48 hr of the [Tc]NGA study.

Technetium-99m NGA functional imaging

The [Tc]NGA studies were divided into two phases: a dynamic phase designed to gather physiologic data, and an imaging phase used to acquire anatomic data. All patients were imaged in the supine position using a commercial gamma camera fitted with a 140 keV (LEAP) collimator. Each patient received 5 mCi of

[Tc]NGA; however, the size of the neoglycoalbumin dose was administered on a per weight basis. Fourteen patients received 7.4×10^{-10} mole of neoglycoalbumin per kg, and four received 18.5×10^{-10} mole per kg. Eight patients received a [Tc]NGA preparation having a carbohydrate density averaging 30 galactose groups per albumin molecule; a preparation averaging 26 galactose per albumin was used in the remaining studies.

Computer† acquisition of gamma camera data was initiated just prior to injection of the radiopharmaceutical. Digital images (128 × 128 pixels) were acquired in byte mode at a rate of 2 frames per min. Two minutes after injection 0.5 ml of blood was sampled and placed in a preweighed plastic tube. The blood concentration of [Tc]NGA was calculated based upon the activity per g of this sample and a diluted standard of the labeled product. Using standard software, time-activity curves were generated for the precordium and liver. Computer acquisition was halted after 30 min and static images (750k–1,000k counts) were acquired. The patient's temperature, pulse, and blood pressure were monitored before and after injection, and at the end of the study.

Kinetic analysis of functional imaging data

Estimates of [HBP] and \bar{Q} were obtained by kinetic analysis of the time-activity data. The kinetic model (9,11) was used to simulate changes in tracer activity in four compartments: systemic blood, hepatic blood, the hepatic parenchyma, and urinary tract. The physiologic parameters which govern the communication between the model compartments were: \bar{Q} , [HBP]; the forward binding rate constant, k_b ; the reverse binding rate constant, k_{-b} ; and a metabolic parameter, α_m . The model assigned the hepatic sinusoidal plasma space as the volume component of the receptor concentration.

The following data was supplied to the model: liver and precordium time-activity data, NGA concentration in the blood at 2 min after injection, a coupling coefficient which converted the [Tc]NGA blood concentration at 2 min to the number of counts in the precordial curve during the 2.0 to 2.5 min interval, and the k_b and k_{-b} for the NGA injected (9). Using standard least-squares techniques (12), estimates for each patient's \bar{Q} and [HBP] were obtained in an automated fashion by matching the simulated curves to the patient's liver and precordial time-activity data. Error propagation of the model has been studied (11) and was used to estimate the coefficient of variation for each parameter estimate.

Assessment of clinical significance

The clinical significance of kinetic parameters, \bar{Q} and [HBP], were evaluated by two methods. The first method was devised to assess their prognostic capability. A normal range was assigned to each parameter: \bar{Q} , 0.30 to 0.40 min^{-1} ; [HBP], $3.0 \times 10^{-6}M$ to $5.0 \times$

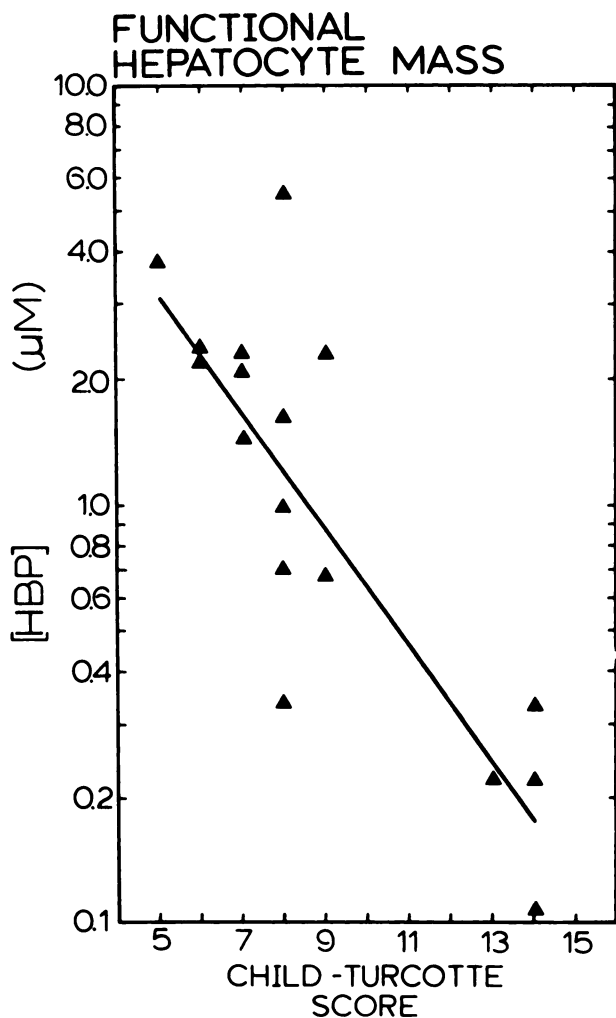


FIGURE 1
Correlation of log[HBP] and Child-Turcotte criteria scores. Excellent correlation is demonstrated ($r_s = -0.72$, $p = 0.001$)

$10^{-6}M$. The range for normal standardized hepatic blood flow, \bar{Q} , was obtained from textbook values for adult \bar{Q} and V . The receptor concentration range was based on the intercept at $X = 5$ of the linear regression line resulting from the plot: CTC score compared with log [HBP] (see Fig. 1). A range representing a depressed [HBP] was also defined: $1.0 \times 10^{-6}M$ to $3.0 \times 10^{-6}M$. The \bar{Q} and [HBP] estimates for each patient were then classified into one of three ranges: \uparrow , above normal; N, normal; \downarrow , depressed; and $\downarrow\downarrow$, severely depressed (Table 1). The patients were separated into three groups: survivors, nonsurvivors, and transplant recipients. No statistical analysis was performed on this data.

The second method was used to evaluate the ability of the [HBP] estimates to provide a quantitative assessment of hepatocellular function. Numerical scores based on Child-Turcotte criteria (CTC) (13) were employed as an independent established index of function-

al hepatocyte mass. Because biological parameters are usually lognormally distributed (14), we compared the logarithm of the [HBP] estimates with the CTC scores. More specifically, one would expect a change in CTC score to produce a proportional rather than an additive change in [HBP]; such relations require logarithmic transformation (15). A linear relationship between log[HBP] and CTC scores would be consistent with our hypothesis that estimates of [HBP] through kinetic analysis of [Tc]NGA time-activity data provide an index of functional hepatocyte mass.

Statistical analysis

The above hypothesis was tested by applying three methods by which the deviation about a linear model may be assessed: (a) Spearman rank correlation (15), which does not assume a normal distribution of either variable; (b) the method of generalized linear models (GLIM) (16), which assumes normally distributed errors with the possibility of nonconstant variance; and (c) least-squares regression analysis (15). The logarithmic transform of the [HBP] estimate was the dependent variable and the CTC score was the independent variable.

RESULTS

Disease distribution

The distribution of liver diseases included seven patients with primary hepatic tumors, eight with hepatic metastases, four with cirrhosis (two of these also had concurrent primary hepatic tumors and one had chronic active hepatitis) and one patient with acute fulminant non-A, non-B hepatitis. The disease distribution, CTC score, [HBP], \bar{Q} , and routine liver function tests are presented in Table 2.

Liver anatomy

Table 3 shows the correlation of [Tc]NGA imaging with other diagnostic imaging modalities: computed tomography (CT), angiography, ultrasonography, and technetium-labeled sulfur colloid ([Tc]SC) imaging. Figure 2 compares [Tc]NGA with [Tc]SC liver images in Patient 1 with hepatocellular carcinoma. In comparing [Tc]SC images to [Tc]NGA, good correlation was seen except in Patient 9 in whom [Tc]NGA imaging demonstrated multiple small lesions throughout the left hepatic lobe that were not detected on the [Tc]SC images. In addition, there was no reticuloendothelial cell uptake (spleen, bone marrow, lung) with [Tc]NGA which provided improved definition of the hepatic anatomy.

In general, the ability of CT imaging and [Tc]NGA imaging to detect lesions was similar. CT imaging usually provided superior anatomical definition. However,

TABLE 1
[Tc]NGA Physiologic Parameters and Clinical Outcome*

Patient no.	[Tc]NGA parameter		Child-Turcotte Score		Interval	Cause of death
	\bar{Q}	[HBP]	At [Tc]NGA study	Subsequent evaluation		
Survivors						
2	N	↓	8	9	10 mo	
5	↓	↓	7	6	4 mo	
8	↓	↑	8	8	6 mo	
12	↓	↓	7	7	9 mo	
14	↓	N	5	9	6 mo	
15	↓	↓	6	5	4 mo	
Nonsurvivors						
1	↓	↓↓	14	15	15 days	Hepatic failure
4	N	↓↓	9	9	2 wk	Widespread metastases
9	↑	↓	7	8	14 mo	Widespread metastases
10	N	↓	7	7	4 mo	Widespread metastases
11	↓	↓	9	10	6 wk	Widespread metastases
13	N	↓↓	8	8	5 mo	Widespread metastases
16	↓	↓↓	14	15	2 wk	Hepatic failure
17	↓	↓↓	13	15	5 wk	Hepatic failure
Liver transplant recipients						
6	↓	↓↓	8			
7	N	↓	6			
18	↓	↓↓	14			

* KEY: Standardized blood flow, \bar{Q} : ↑ = > 0.40 min⁻¹; N = 0.30 - 0.40 min⁻¹; ↓ = < 0.30 min⁻¹. HBP concentration, [R]: ↑ = > 5.0 × 10⁻⁶M; N = 3.0 - 5.0 × 10⁻⁶M; ↓ = 1.0 - 3.0 × 10⁻⁶M; ↓↓ = < 1.0 × 10⁻⁶M.

in Patient 6 multiple diffuse lesions were demonstrated by [Tc]NGA imaging which were not detected by CT imaging with and without i.v. contrast enhancement. Pathologic examination of this patient's liver after hepatic transplantation revealed massive hepatomegaly (6,030 g) with diffuse, multifocal involvement by hepatocellular carcinoma. In general, angiography also provided superior spatial resolution; however, in Patient 11, a diffusely infiltrating hypovascular neoplasm tumor size and distribution was better demonstrated by [Tc]NGA. Good correlation was obtained between [Tc]NGA imaging and ultrasonography.

Liver function

Table 1 contains a comparison between the two [Tc]NGA physiologic parameters (\bar{Q} , [HBP]), and patient clinical outcome. Marked decreases in [HBP] (concentrations less than 1 × 10⁻⁶M) were seen only in nonsurviving patients. All three patients who died with hepatic failure demonstrated a combination of decreased \bar{Q} (< 0.3 min⁻¹), and a markedly decreased [HBP] (< 1 × 10⁻⁶M).

Figure 3 contains hepatic time-activity curves from three patients with varying degrees of hepatic dysfunction. These curves demonstrate large changes in the rate of hepatic [Tc]NGA uptake, which indicates the

sensitivity of [Tc]NGA kinetics to hepatic dysfunction.

Clinical correlation

Brief case histories of these three patients are included to provide clinical correlation of the results.

Patient 1 (hepatoma/cirrhosis/chronic active hepatitis)

This 36-yr-old male with a prior history of chronic active hepatitis and cirrhosis was admitted for progressive jaundice, malaise, and lethargy. On physical examination he appeared moderately cachectic and had scleral icterus. Abdominal examination disclosed a firm and slightly tender liver without splenomegaly or ascites. His hepatic encephalopathy and ascites were well controlled with medical therapy. Laboratory values included: bilirubin 4.7 mg/dl, albumin 2.2 g/dl, alkaline phosphatase 277 U/l, serum glutamicoxaloacetic transaminase (SGOT) 152 U/l. Technetium-99m SC imaging disclosed a large lesion in the dome of the right lobe of the liver, which was also detected by the Tc-NGA study (Fig. 2). Analysis of the kinetic data (Fig. 3) provided a low value for \bar{Q} , 0.12 ± 0.04 min⁻¹, and a markedly low value for [HBP], 0.34 ± 0.51 μM. The patient was placed on chemotherapy but died due to hepatic failure 2 wk after [Tc]NGA imaging.

TABLE 2
Clinical Summary

Patient no.*	Age (yr)	Primary diagnosis [†]	Child-Turcotte Score	Parameter estimates [‡]		Laboratory values				
				\bar{Q} (min^{-1})	[HBP] (μM)	billi (mg/dl)	Alb (g/dl)	PT [¶] (sec)	SGOT (U/l)	Alk. Phos. (U/l)
Group I—Primary hepatic tumors										
1	36	Hepatoma/cirrhosis/CAH	14	0.12(0.30)	0.34(1.52)	4.7	2.2	22.0	152	277
2	53	Hepatoma	8	0.30(0.07)	1.6 (0.56)	1.4	2.6	13.1	82	457
3	66	Hepatoma	7	NA	NA	0.7	4.3	11.9	50	212
4	56	Hepatoma	9	0.39(0.05)	0.69(0.12)	2.6	2.4	13.0	390	1191
5	29	Hepatoma	7	0.08(0.17)	2.2 (0.13)	1.1	2.7	12.9	250	170
6	43	Hepatoma	8	0.16(0.09)	0.31(0.25)	0.5	3.8	11.1	312	1023
7	22	Hepatoma	6	0.37(0.14)	2.1 (0.36)	0.4	3.9	10.2	69	83
Group II—Hepatic metastases										
8	52	Common bile duct carcinoma	8	0.20(0.03)	5.5 (0.41)	6.1	3.2	12.6	83	884
9	39	Breast carcinoma	7	0.46(0.18)	1.2 (0.42)	0.6	3.4	10.6	27	370
10	53	Ovarian carcinoma	7	0.31(0.09)	2.1 (0.56)	0.1	3.9	9.5	18	370
11	63	Endometrial carcinoma	9	0.22(0.09)	2.3 (0.66)	15.8	3.3	13.0	142	756
12	88	Unknown primary tumor	7	0.21(0.02)	1.3 (0.63)	0.2	4.2	11.9	12	257
13	53	Colon carcinoma	8	0.31(0.07)	0.96(0.26)	1.1	3.1	11.0	51	840
14	55	Stomach leiomyosarcoma	5	0.25(0.05)	3.8 (0.70)	1.1	2.7	12.7	48	271
15	58	Carcinoid	6	0.15(0.21)	2.4 (1.26)	0.2	3.5	10.6	60	223
Group III—Cirrhosis										
16	46	Postnecrotic cirrhosis	14	0.02(0.44)	0.08(2.80)	4.3	2.3	14.6	24	120
17	48	Chronic active hepatitis	13	0.05(0.04)	0.22(0.08)	2.3	2.7	12.9	33	147
1	36	Cirrhosis/hepatoma/CAH	14	0.12(0.30)	0.34(1.52)	4.7	2.2	22.0	152	277
3	66	Cirrhosis/hepatoma	7	NA	NA	0.7	4.3	11.9	50	212
Group IV—Acute fulminant hepatitis										
18	36	Acute fulminant non-A non-B hepatitis	14	0.06(3.50)	0.22(2.51)	32.0	2.5	19.4	98	369

* Patients No. 4, 5, 6, and 17 received 18.5×10^{-10} mole [Tc]NGA/kg of body weight; remaining patients received 7.4×10^{-10} mole/kg. Patients No. 1-3, 8-12 received [Tc]NGA-30 (30 galactose/HSA); remaining patients received [Tc]NGA-26.

[†] All diagnoses established by histologic examination of liver.

[‡] Coefficient of variation in parenthesis.

[¶] Prothrombin time.

Patient 2 (hepatoma)

This 53-yr-old male presented with complaints of right upper quadrant pain, anorexia, and nausea. Physical examination revealed a well-nourished male without evidence of muscular wasting. Scleral icterus was absent and abdominal examination revealed an enlarged, slightly tender liver and absence of ascites. Asterixis was absent and no abnormalities were noted on neurological examination. Laboratory studies at the time of the [Tc]NGA study included: bilirubin 1.4 mg/dl, albumin 2.6 g/dl, alkaline phosphatase 457 U/l, and (SGOT) 82 U/l. A CT scan of the liver demonstrated multiple low-density masses throughout both lobes which were seen as cold defects on the

[Tc]NGA study. Kinetic analysis of the [Tc]NGA data (Fig. 3) provided normal values for \bar{Q} and [HBP], $0.30 \pm 0.02 \text{ min}^{-1}$ and $1.6 \pm 0.9 \mu\text{M}$, respectively (Table 2). Liver biopsy revealed hepatocellular carcinoma. Additional biopsies taken from areas adjacent to the tumor mass revealed a normal histologic pattern. The patient subsequently underwent chemotherapy with good response and is alive 10 mo after the [Tc]NGA study.

Patient 16 (postnecrotic cirrhosis)

This 46-yr-old male was admitted with complaints of lethargy, and abdominal and ankle swelling. Physical examination revealed marked icterus with severe muscle

TABLE 3
Comparison of [Tc]NGA Functional Imaging and Other Diagnostic Imaging Modalities*

I. Computed tomography

Patient no.	Liver size NGA/CT	Lesion no. NGA/CT	Lesion size NGA/CT	Lesion distribution NGA/CT
1	N/N	2/1	L/L	L/T
2	E/E	M/M	L/L	D/D
3	E/E	M/M	S,M,L/S,M,L	D/D
5	E/E	M/M	S,M,L/S,M,L	D/D
6	E/E	M/O	S,M,L/O	D/O
7	N/N	1/2	L/S,L	C/L
8	E/N	2/1	S,L/L	T/T
10	N/N	1/2	S/S,M	L/D
12	N/N	2/2	S/S,M	T/T
13	E/E	M/M	S,M,L/S,M,L	D/D
14	E/E	M/M	S,M,L/S,M,L	D/D
15	N/N	0/0		
16	S/S	0/0		
18	S/S	0/0		

II. Selective angiography

Patient no.	Liver size NGA/Angio	Lesion no. NGA/Angio	Lesion size NGA/Angio	Lesion distribution NGA/Angio
1	N/N	2/1	L/L	L/T
6	E/E	M/M	S,M,L/S,M,L	D/D
11	N/N	1/Ind	S/L	L/T
16	S/Ind	0/Ind		
17	W/N	1/2	L/M,L	C/C

III. Ultrasound

Patient no.	Liver size NGA/US	Lesion no. NGA/US	Lesion size NGA/US	Lesion distribution NGA/US
1	E/E	M/M	S,M,L/S,M,L	D/D
3	E/E	M/M	S,M,L/S,M,L	D/D
8	E/E	2/2	S,L/S,L	T/T
12	N/N	2/2	S/M	T/T

IV. [Tc]SC hepatic scintigraphy

Patient no.	Liver size NGA/SC	Lesion no. NGA/SC	Lesion size NGA/SC	Lesion distribution NGA/SC
1	N/N	2/2	L/L	L/T
3	E/E	M/M	S,M,L/S,M,L	D/D
8	E/E	2/2	S,L/S,L	T/T
9	N/N	M/3	S/S	D/T

* KEY: Liver size: S = small; N = normal; E = enlarged. Lesion no.: 0 = none; M = multiple; Ind = indeterminate. Lesion size: S = small, less than 3 cm diam; M = medium, 3-6 cm; L = large, greater than 6 cm diam. Lesion distribution: S = segmental or localized; L = lobar (right or left); T = trisegmental (right or left); C = central (left median and right anterior segments); D = diffuse.

wasting. Tense ascites and splenomegaly were present on abdominal exam, and the liver could not be ballotated. Asterixis, apathy, and disorientation were present

on neurological examination. Laboratory values at the time of the [Tc]NGA study included: bilirubin 4.3 mg/dl, albumin 2.3 g/dl, alkaline phosphatase 120 U/l, SGOT 24 U/l, and prothrombin time 14.6 sec/control 11.2 sec. Liver biopsy revealed chronic active hepatitis with end-stage cirrhosis. Technetium-99m NGA imaging demonstrated a small, shrunken liver with patchy distribution of the tracer. The hepatic time-activity curve demonstrated markedly decreased uptake (Fig. 3). Kinetic analysis demonstrated a decreased \bar{Q} , $0.018 \pm 0.008 \text{ min}^{-1}$, and a severely diminished [HBP] $0.08 \pm 0.22 \mu\text{M}$. Two weeks after the [Tc]NGA study the patient was readmitted with severe encephalopathy, ascites, and hepatorenal syndrome. He expired shortly after admission.

Statistical analysis

The linear association of the CTC scores and the log of the [HBP] estimates (Fig. 1) was confirmed by all three methods. Spearman rank correlation analysis produced a coefficient r_s of -0.72 ($df = 15$, $p = 0.001$). Analysis by GLIM revealed a significant relationship by maximum likelihood testing: mean-squared error = 0.73 , $p = 0.001$. Standard linear least-squares regression also revealed a strong correlation ($r = -0.85$, $p < 0.001$). Based on the above results we rejected our null hypothesis, and concluded that the logarithm of the [HBP] parameter was a measure of functional hepatocyte mass.

DISCUSSION

Liver anatomy

Initial clinical experience with [Tc]NGA liver imaging indicates that this technique provides anatomic information of comparable diagnostic quality to that obtained with other imaging modalities. In comparison to CT imaging and angiography, [Tc]NGA, like [Tc]SC scintigraphy, has some limitations in its ability to spatially discriminate hepatic lesions in terms of individual lesion size and distribution. Significant improvement in anatomical definition may be obtained by application of single photon emission computed tomographic (SPECT) imaging. Technetium-99m NGA imaging, in contrast to [Tc]SC imaging, provided excellent hepatic images in patients with severe hepatocellular dysfunction, since extrahepatic uptake did not occur.

Also, in contrast to currently used technetium-labeled hepatobiliary agents (iminodiacetic acid derivatives), uptake of native HBP ligands, and hence [Tc]NGA, are unaffected by high serum bilirubin levels, or bile salts (17). This occurs since its uptake is mediated by an independent biochemical process (18).

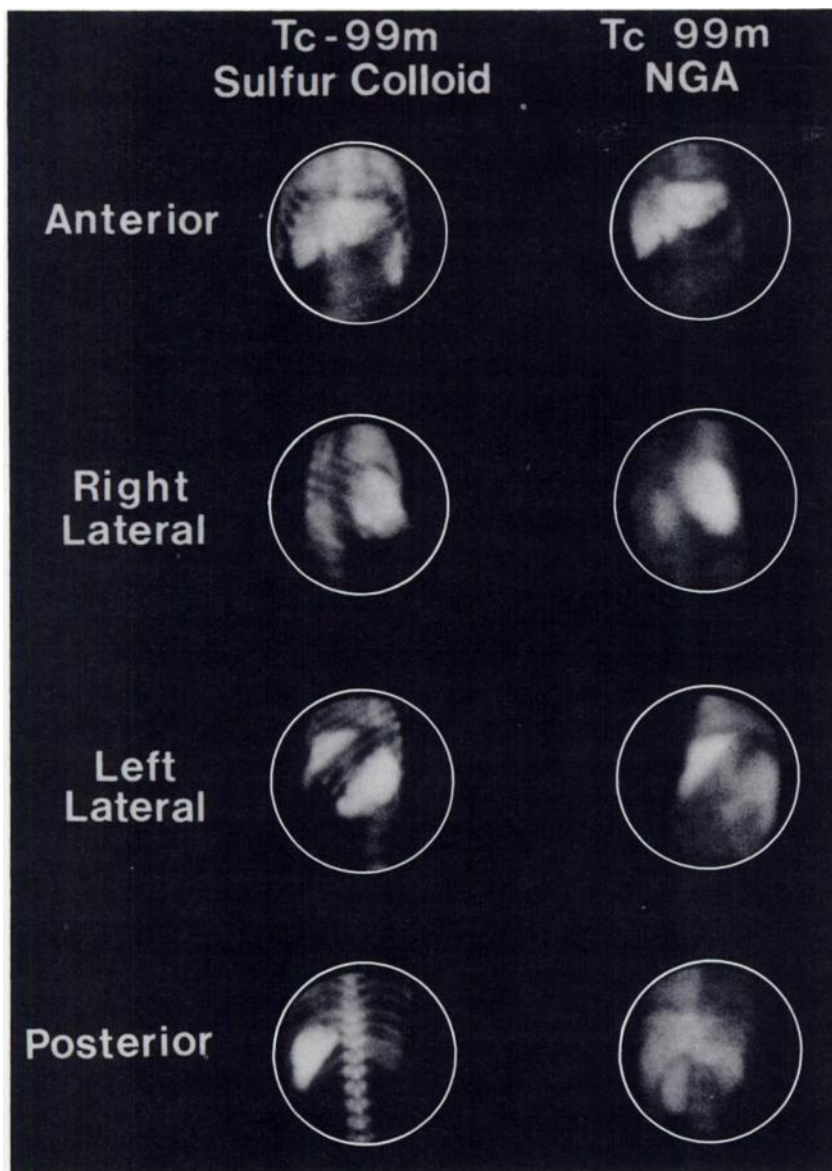


FIGURE 2
 Patient 1 Composite image comparing [Tc]SC to [Tc]NGA. Patient was 30-yr-old male with hepatoma superimposed upon chronic active hepatitis and cirrhosis. [Tc]NGA (5.3 mCi, 196 MBq) was injected intravenously and images obtained at 1 hr. There is large lesion in dome of right lobe of liver which was more easily visualized on [Tc]NGA study. Extrahepatic activity on [Tc]NGA study is due to persistence of free [Tc]NGA in blood (measured at 55% of injected dose at 30 min) in this patient with severely depressed hepatic functional reserve

In the present studies, one patient with moderately well-preserved hepatic function (Patient 11), demonstrated good hepatic uptake and excellent imaging anatomy despite marked hyperbilirubinemia (bilirubin 15.8 mg/dl).

Liver function

The uniqueness of [Tc]NGA imaging lies in its ability to provide information regarding hepatic function, specifically [HBP] and \bar{Q} (Table 2). Changes in either of these two independent physiologic parameters are reflected in the rate of hepatic uptake of [Tc]NGA. Delivery of [Tc]NGA is determined by the magnitude of the hepatic blood flow, and the rate of the receptor-mediated binding process is governed by the affinity of [Tc]NGA for the receptor and by [HBP]. Thus, changes in \bar{Q} and [HBP] will be reflected as changes in

the shape of the liver time-activity curves. For example, a decrease in receptor concentration will produce a liver time-activity curve with a decreased slope, and a delay in the time at which the curve peaks.

The clinical significance of \bar{Q} and [HBP] was tested by comparison with CTC (13), the most widely used means for assessment of functional hepatocyte mass (19,20). Comparison of \bar{Q} and CTC scores demonstrated lower values for \bar{Q} in patients with high CTC scores (Table 2). Our results, in agreement, with flow measurements obtained by other methods (21,22), demonstrate decreased perfusion in the presence of advanced hepatocellular disease.

In vivo estimates of HBP concentration provide a new means for evaluating functional hepatocyte mass. The evidence in this study indicates that [Tc]NGA uptake is sensitive to clinical and histologic manifesta-

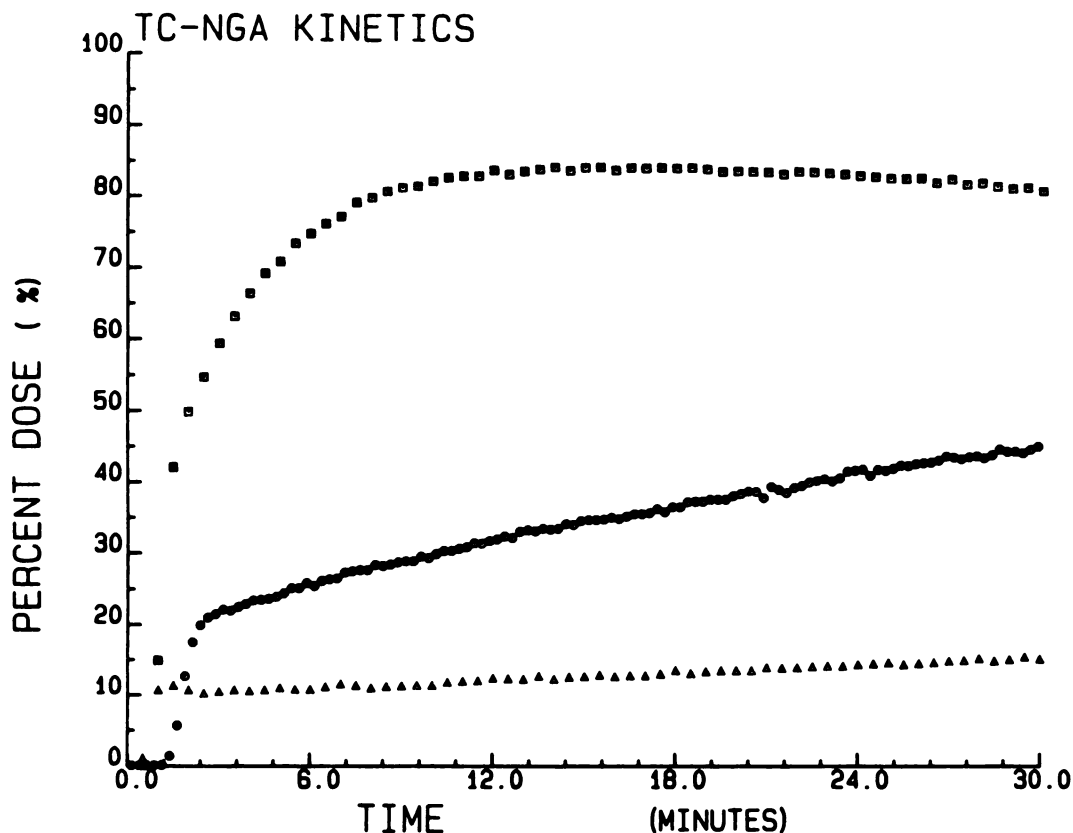


FIGURE 3

Liver time-activity curves from three patients. Each curve is scaled (7) to percentage of [Tc]NGA residing within liver. Curves which have longer times and diminished peak heights are indicative of poor hepatic function; i.e., reduced \bar{Q} and/or decreased [HBP]. Patients 1 and 16 expired within weeks after the [Tc]NGA study. (□) #2 hepatoma, normal liver; (○) #1 hepatoma, CAH, cirrhosis; (△) #16 CAH, cirrhosis

tions of liver disease. The three hepatic time-activity curves in Fig. 3 demonstrate large variations in the rate of [Tc]NGA uptake between Patient 2 (see case history) and two patients with severe hepatocellular necrosis (see case histories for Patients 1 and 16). Further evidence was established by comparing [HBP] with CTC scores (Fig. 1). The high correlation obtained in this comparison ($r_s = -0.72$) indicates that [HBP] is directly related to the clinical and biochemical manifestations of reduced functional hepatocyte mass. This corresponds to recent measurements of labeled-asialoglycoprotein uptake by rat liver and in vitro membrane binding using experimental models representing hepatitis (23,24).

The patient survival data is evidence that [Tc]NGA imaging may provide prognostic information: patients with decreased \bar{Q} and markedly decreased [HBP] died in hepatic failure within 6 wk of the [Tc]NGA study. Patients without this combination did not die of hepatic failure (Table 1). None of the patients with a markedly decreased [HBP] survived more than 5 mo after the [Tc]NGA imaging study. All currently surviving patients had either a normal or mildly decreased [HBP].

Additional experience will define more clearly the prognostic capabilities of [Tc]NGA functional imaging.

Significance

Since standard liver function tests are of limited value (25) a quantitative test of functional hepatocyte mass could significantly enhance the diagnosis and management of liver disease. Technetium-99m NGA may provide a noninvasive means for selection of medical or surgical management in patients with portal hypertension and esophageal variceal hemorrhage. Serial [Tc]NGA studies may document changes in hepatocellular function in patients undergoing therapy for chronic active hepatitis and provide a prognostic index in patients with fulminant hepatitis. Serial measurements of \bar{Q} and [HBP] by way of [Tc]NGA imaging may also provide a means for evaluation of hepatic function in patients undergoing therapy for hepatic tumors.

In addition to its potential for clinical application, by virtue of its high tissue specificity, the [Tc]NGA-HBP system will also serve as a model for the development of

in vivo quantitation of receptor biochemistry via kinetic modeling. These studies can lead to: (a) clearer understanding of hepatic drug elimination; (b) refinement of therapeutic techniques such as radioimmunotherapy, as well as, (c) increased diagnostic potential of other receptor-binding radiotracers.

Receptor-binding radiopharmaceuticals provide a new tracer method by which other organ systems and disease processes may be studied. Technetium-99m is the most convenient radionuclide for nuclear medicine procedures and current detection systems are optimized to its physical characteristics. In addition, the kinetic analysis of [Tc]NGA imaging data executes in a standard nuclear medicine computer. In light of these considerations and this preliminary clinical experience, [Tc]NGA imaging provides a valuable and also practical new tool for the noninvasive evaluation of liver disease.

CONCLUSION

Technetium-99m NGA hepatic functional imaging is a new technique which has considerable clinical and research potential. Initial clinical studies with this new agent have demonstrated its functional and anatomic imaging capabilities. Technetium-99m NGA appears to be the first receptor-binding radiopharmaceutical with potential for broad clinical application, that is, the measurement of functional hepatocyte mass.

FOOTNOTES

* Cutter Laboratories, Plasbumin-25, Berkeley, CA.

† ADAC Laboratories, DPS-2800, San Jose, CA.

ACKNOWLEDGMENTS

The authors are indebted to Dr. Robert Quadro and Dr. James Goodnight for their participation and patient referrals; to Dr. Paul Scheibe for reviewing the kinetic data; Marijane Krohn for performing the GLIM and LS regression analysis; and Dusan Hutak for his excellent technical assistance.

This work was presented at the 31st Annual Meeting of the Society of Nuclear Medicine, Los Angeles, CA, June 5-8, 1984 and was supported by a grant (#PDT-180) from the American Cancer Society, and The Fred and Julia Rusch Foundation. Dr. Stadalnik is a James Picker Foundation Scholar. Dr. Woodle was supported in part by a grant (GM-07860) from the United States Public Health Service.

REFERENCES

- Eckelman WC, Reba RC, Gibson RE, et al: Receptor-binding radiotracers: A class of potential radiopharmaceuticals. *J Nucl Med* 20:350-357, 1979
- Neufeld EF, Ashwell G: Carbohydrate recognition systems for receptor-mediated pinocytosis. In *The Biochemistry of Glycoproteins and Proteoglycans*, Lenarz WJ, ed. New York, Plenum Publishing, 1980, pp 241-266
- Stockert RJ, Morell AG: Hepatic binding protein: The galactose-specific receptor of mammalian hepatocytes. *Hepatology* 3:750-757, 1983
- Gärtner U, Stockert RJ, Morell AG, et al: Modulation of the transport of bilirubin and asialoorosomucoid during liver regeneration. *Hepatology* 2:99-106, 1981
- Stockert RJ, Becker FF: Diminished hepatic binding protein for desialylated glycoproteins during chemical hepatocarcinogenesis. *Cancer Res* 40:3632-3634, 1980
- Collins JC, Stockert RJ, Morell AG: Asialoglycoprotein receptor expression in murine pregnancy and development. *Hepatology* 4:80-83, 1984
- Vera DR, Stadalnik RC, Krohn KA: Tc-99m Galactosyl-neoglycoalbumin: Preparation and preclinical studies. *J Nucl Med* 26:1157-1167, 1985
- Vera DR, Krohn KA, Stadalnik RC, et al: Tc-99m-galactosyl-neoglycoalbumin: In vivo characterization of receptor-mediated binding to hepatocytes. *Radiology* 151:191-196, 1984
- Vera DR, Krohn KA, Stadalnik RC, et al: Tc-99m-galactosyl-neoglycoalbumin: *In vitro* characterization of receptor-mediated binding. *J Nucl Med* 25:779-787, 1984
- Benjamin PP: A rapid and efficient method of preparing Tc-99m-human serum albumin: Its clinical applications. *Int J Appl Radiat Isot* 20:187-194, 1969
- Vera DR, Krohn KA, Scheibe PO, Stadalnik RC: Identifiability analysis of an *in vivo* receptor-binding radiopharmacokinetic system. *IEEE Trans Biomed Eng BME-32:312-322*, 1985
- Lawson CL, Hanson RJ: *Solving Least Squares Problems*, Englewood Cliffs, NJ, Prentice-Hall, 1974
- Child III CG, Turcotte JG: Surgery and portal hypertension. In *The Liver and Portal Hypertension*, Child CG III, ed. Philadelphia, W.B. Saunders, 1964, pp 1-85
- Aithchison J, Brown JAC: *The Lognormal Distribution*, Boston, Cambridge University Press, 1957
- Snedecor GW, Cochran WG: *Statistical Methods*, 6th ed. Ames, Iowa, The Iowa State University Press, 1967
- McCullagh P, Nelder JA: *Generalized Linear Models*, New York, Chapman and Hall, 1983
- Russel FGM, Weitering JG, Oosting R, et al: Influence of taurocholate on hepatic clearance and biliary excretion of asialo intestinal alkaline phosphatase in the rat in vivo and in isolated perfused rat liver. *Gastroenterology* 85:225-234, 1983
- Stockert RJ, Gärtner U, Morell AG, et al: Effects of receptor-specific antibody on the uptake of desialylated glycoproteins in the isolated perfused rat liver. *J Biol Chem* 255:3830-3831, 1980
- Conn HO: A peek at the Child-Turcotte classification. *Hepatology* 1:673-676, 1981
- Christensen E, Schlichting P, Fauerholdt L, et al: Prognostic value of Child-Turcotte Criteria in medically treated cirrhosis. *Hepatology* 4:430-435, 1984
- Bradley S, Ingelfinger F, Bradley G: Hepatic circulation in cirrhosis. *Circulation* 5:419-429, 1952
- Vetter H, Falkner R, Neumayr A: The disappearance rate of colloidal radiogold from the circulation and its application to the estimation of liver blood flow in normal and cirrhotic subjects. *J Clin Invest* 33:1594-1602, 1954
- Wong MWC, Jamieson JC: Evidence for reduced up-

- take of asialo- α_1 -acid glycoprotein during the acute phase response to inflammation. *Life Sci* 25:827-834, 1979
24. Sawamura T, Kawasato S, Shiozaki Y, et al: Decrease of a hepatic binding protein specific for asialoglycoproteins with accumulation of serum asialoglycoproteins in galactosamine-treated rats. *Gastroenterology* 81: 527-533, 1981
25. McIntyre N: Limitations of conventional liver function tests. *Semin Liver Dis* 3:265-274, 1983